

# CHEMISTRY OF MATERIALS

VOLUME 18, NUMBER 6

MARCH 21, 2006

© Copyright 2006 by the American Chemical Society

## Communications

### Covalent Assembled Osmium-Chromophore-Based Monolayers: Chemically Induced Modulation of Optical Properties in the Visible Region

Tarkeshwar Gupta, Marc Altman, Atindra D. Shukla, Dalia Freeman, Gregory Leitus, and Milko E. van der Boom\*

Department of Organic Chemistry, Weizmann Institute of Science, 76100 Rehovot, Israel

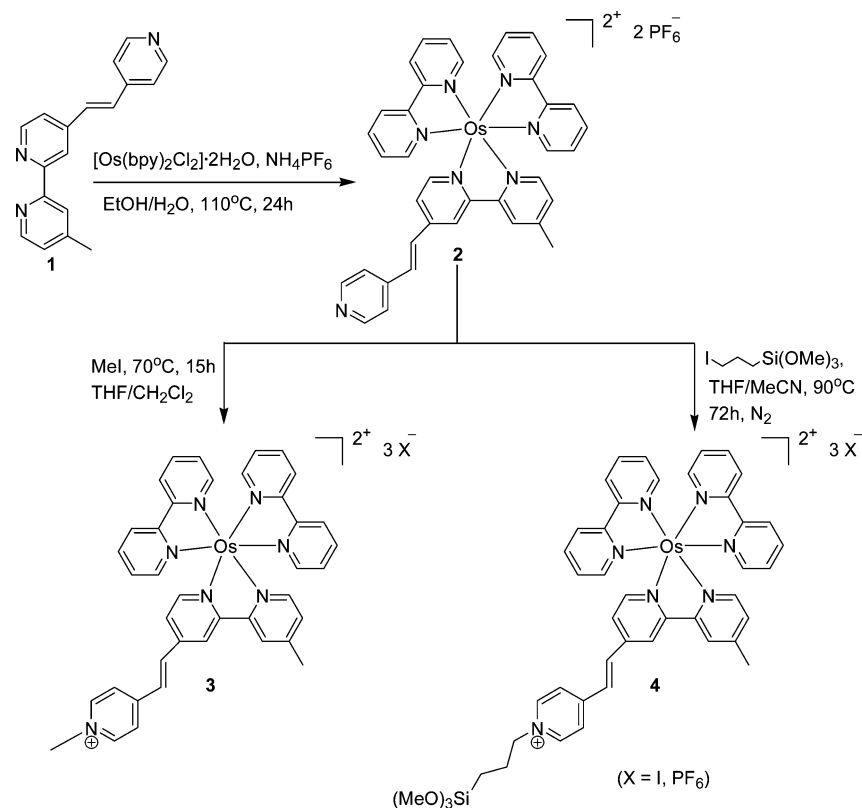
Received October 26, 2005

Monolayer chemistry and surface engineering, in particular the assembly of new molecular-based electronic, electrooptic, and photonic materials, is a fast emerging field.<sup>1</sup> Controlling and switching of monolayer molecular properties is of much relevance for the design and formation of prototype organic nanodevices,<sup>2–4</sup> including memory elements,<sup>5–7</sup> sensors,<sup>8</sup>

optical switches,<sup>9</sup> and logic architectures.<sup>2,10</sup> Numerous molecular switches have been reported and are often based on either photo- or electro-induced processes associated with reversible structural changes in solution or in liquid crystals.<sup>4,11,12</sup> Monolayer-based memory elements and switches are of much current interest.<sup>4,5–7,9,13</sup> Robust metal complexes are suitable candidates as molecular building blocks for the formation of monolayer-based memory elements and switches by virtue of the dominating electronic and optical properties

\* To whom correspondence should be addressed. E-mail: milko.vanderboom@weizmann.ac.il.

- (1) (a) van der Boom, M. E.; Marks, T. J. *Polymers for Microelectronics and Nanoelectronics. ACS Symp. Ser.* **2004**, *874*, 30–43. (b) Salomon, A.; Cahen, D.; Lindsay, S.; Tomfohr, J.; Engelkes, V. B.; Frisbie, C. D. *Adv. Mater.* **2003**, *15*, 1881–1890. (c) van der Boom, M. E. *Angew. Chem., Int. Ed.* **2002**, *41*, 3363–3366. (d) Gittins, D. I.; Bethell, D.; Schiffrin, D. J.; Nichols, R. J. *Nature* **2000**, *408*, 67–69. (e) Feldheim, D. *Nature* **2000**, *408*, 45–46. (f) Yerushalmi, R.; Sherz, A.; van der Boom, M. E.; Kraatz, H.-B. *J. Mater. Chem.* **2005**, *15*, 4480–4487.
- (2) Raymo, F. M. *Adv. Mater.* **2002**, *14*, 401–414.
- (3) Nitahara, S.; Akiyama, T.; Inoue, S.; Yamada, S. *J. Phys. Chem. B* **2005**, *109*, 3944–3948.
- (4) Lahann, J.; Mitragotri, S.; Tran, T.-N.; Kaido, H.; Sundaram, J.; Choi, I. S.; Hoffer, S.; Somorjai, G. A.; Langer, R. *Science* **2003**, *299*, 371–374.
- (5) (a) Chen, J.; Ma, D. *Appl. Phys. Lett.* **2005**, *87*, 023505/023501–023505/023503. (b) Liu, Z.; Yasserli Amir, A.; Lindsey, S.; Bocian David, F. *Science* **2003**, *302*, 1543–1545. (c) Roth, K. M.; Yasserli, A. A.; Liu, Z.; Dabke, R. B.; Malinovsky, V.; Schweikart, K.-H.; Yu, L.; Tiznado, H.; Zaera, F.; Lindsey, J. S.; Kuhr, W. G.; Bocian, D. F. *J. Am. Chem. Soc.* **2003**, *125*, 505–517.
- (6) Shukla, A. D.; Das, A.; van der Boom, M. E. *Angew. Chem., Int. Ed.* **2005**, *44*, 3237–3240.
- (7) (a) Sortino, S.; Di Bella, S.; Conoci, S.; Petralia, S.; Tomasulo, M.; Paccial, E. J.; Raymo, F. M. *Adv. Mater.* **2005**, *17*, 1390–1393. (b) Sortino, S.; Petralia, S.; Conoci, S.; Di Bella, S. *J. Am. Chem. Soc.* **2003**, *125*, 1122–1123. (c) Sortino, S.; Petralia, S.; Conoci, S.; Di Bella, S. *Mater. Sci. Eng., C* **2003**, *23*, 857–860.
- (8) (a) Bronson, R. T.; Michaelis, D. J.; Lamb, R. D.; Hussein, G. A.; Farnsworth, P. B.; Linford, M. R.; Izatt, R. M.; Bradshaw, J. S.; Savage, P. B. *Org. Lett.* **2005**, *7*, 1105–1108. (b) Gulino, A.; Mineo, P.; Scamporrino, E.; Vitalini, D.; Fragalà, I. *Chem. Mater.* **2004**, *16*, 1838–1840. (c) Ye, S.; Zhou, W.; Abe, M.; Nishida, T.; Cui, L.; Uosaki, K.; Osawa, M.; Sasaki, Y. *J. Am. Chem. Soc.* **2004**, *126*, 7434–7435. (d) Shipway, A. N.; Katz, E.; Willner, I., *ChemPhysChem* **2000**, *1*, 18–52.
- (9) (a) Yasutomi, S.; Morita, T.; Kimura, S. *J. Am. Chem. Soc.* **2005**, *127*, 14564–14565. (b) Jiang, W.; Wang, G.; He, Y.; Wang, X.; An, Y.; Song, Y.; Jiang, L. *Chem. Commun.* **2005**, 3550–3552. (c) Yasutomi, S.; Morita, T.; Imanishi, Y.; Kimura, S. *Science* **2004**, *304*, 1944–1947. (d) Sortino, S.; Petralia, S.; Conoci, S.; Di Bella, S. *J. Mater. Chem.* **2004**, *14*, 811–813. (e) Ichimura, K.; Oh, S.-K.; Nakagawa, M. *Science* **2000**, *288*, 1624–1626. (f) Stiller, B.; Knochenhauer, G.; Markava, E.; Gustina, D.; Muzikante, I.; Karageorgiev, P.; Brehmer, L. *Mater. Sci. Eng., C* **1999**, *8–9*, 385–389.
- (10) (a) de Silva, A. P.; McClenaghan, N. D. *Chem.—Eur. J.* **2004**, *10*, 574–586. (b) Callan, J. F.; de Silva, A. P.; McClenaghan, N. D. *Chem. Commun.* **2004**, 2048–2049.
- (11) (a) Asselberghs, I.; Clays, K.; Persoons, A.; Ward, M. D.; McCleverty, J. J. *Mater. Chem.* **2004**, *14*, 2831–2839. (b) Coe, B. J. *Chem.—Eur. J.* **1999**, *5*, 2464–2471. (c) Coe, B. J.; Houbrechts, S.; Asselberghs, I.; Persoons, A. *Angew. Chem., Int. Ed.* **1999**, *38*, 366–369.
- (12) (a) Luk, Y.-Y.; Abbott, N. L. *Science* **2003**, *301*, 623–626. (b) Kalny, D.; Elhabiri, M.; Moav, T.; Vaskevich, A.; Rubinstein, I.; Shanzer, A.; Albrecht-Gary, A.-M. *Chem. Commun.* **2002**, 1426–1427. (c) de Silva, A. P.; Fox, D. B.; Moody, T. S.; Weir, S. M. *Trends Biotechnol.* **2001**, *19*, 29–34. (d) Zelikovich, L.; Libman, J.; Shanzer, A. *Nature* **1995**, *374*, 790–792.

Scheme 1. Formation of Model Complex **3** and the Analogous Molecular Building Block **4** (bpy = 2,2'-Bipyridine)

associated with the metal center. For instance, Di Bella et al. successfully addressed the optical properties of a ruthenium-chromophore-based monolayer bound to transparent platinum electrodes via a thiol moiety.<sup>7</sup> In addition, electrochemical control of the optical properties of a ruthenium-complex-based monolayer in the UV region has been reported.<sup>6</sup> Here we report on the chemical modulation of the optical absorbance in the entire visible region (400–750 nm) of a well-defined, thermally robust siloxane-based monolayer as a function of the metal oxidation state of a dipolar osmium-based chromophore.

Reaction of  $\text{Os}(\text{2,2}'\text{-bipyridine})_2\text{Cl}_2 \cdot 2\text{H}_2\text{O}$ <sup>14</sup> with 1.2 equiv of 4'-methyl-4-(2-pyridin-4-yl-vinyl)-[2,2']bipyridine<sup>15</sup> (**1**) in ethanol/water (1:1, v/v) under reflux for 24 h followed by addition of an excess of a saturated aqueous solution of  $\text{NH}_4\text{PF}_6$  affords the new complex **2** (Scheme 1). Reaction of **2** with an excess of  $\text{MeI}$  in tetrahydrofuran ( $\text{THF}/\text{CH}_2\text{Cl}_2$  (9:1, v/v) at  $70^\circ\text{C}$  for 15 h resulted in the formation of the corresponding pyridinium salt **3**. Reaction of complex **2** with an excess of 3-iodo-*n*-propyl-1-trimethoxysilane in dry  $\text{THF}/\text{acetonitrile}$  (9:1, v/v) under  $\text{N}_2$  in a pressure vessel at  $90^\circ\text{C}$  for 72 h resulted in the formation of pyridinium salt **4**. The new  $d^6$  osmium(II) complexes **2–4** were isolated in good yields and fully characterized by a combination of  $^1\text{H}$  and  $^{13}\text{C}\{^1\text{H}\}$  NMR spectroscopy, UV/vis spectroscopy, mass

spectrometry, and elemental analyses. In addition, complex **3** has been structurally characterized by single crystal X-ray crystallography unambiguously confirming the six coordinate octahedral geometry around the metal center and the formation of the pyridinium moiety (Figure 1).

The ruthenium analogue of complex **2** has recently been reported.<sup>16</sup> The appearance of singlet and triplet signals at  $\delta$  4.26 and  $\delta$  4.46 in the  $^1\text{H}$  NMR spectra of complexes **3** and **4**, respectively, is typical for the quaternization of a pyridine moiety.<sup>17</sup> The UV/vis spectra of complexes **3** and **4** in dry acetonitrile showed red shifts of  $\Delta\lambda = +23$  nm and  $+18$  nm for the metal-to-ligand charge transfer ( $^1\text{MLCT}$ ) bands, respectively, in comparison to the  $^1\text{MLCT}$  band of complex **2** with  $\lambda_{\text{max}} = 487$  nm. A red shift is expected for the formation of pyridinium salts.<sup>17</sup> Coordinatively saturated trisbipyridyl complexes are known to be thermally robust and often exhibit reversible redox properties.<sup>14,18</sup>

Robust siloxane-based monolayers are formed by covalent assembly of complex **4** from solution on glass and  $\text{Si}(100)$  substrates (Figure 2). Freshly cleaned glass and silicon substrates were fully immersed in a dry acetonitrile/toluene (3:7, v/v) solution of complex **4** (0.5 mM) under  $\text{N}_2$  and heated for 52 h at  $85^\circ\text{C}$  using glass pressure vessels with the exclusion of light. Subsequently, the functionalized substrates were rinsed thoroughly and sonicated with acetonitrile and 2-propanol for 6 min to remove physisorbed

(13) (a) Chi, Y. S.; Hwang, S.; Lee, B. S.; Kwak, J.; Choi, I. S.; Lee, S.-G. *Langmuir* **2005**, *21*, 4268–4271. (b) Liu, Y.; Mu, L.; Liu, B.; Kong, J. *Chem.—Eur. J.* **2005**, *11*, 2622–2631. (c) Sortino, S.; Petralia, S.; Di Bella, S. *J. Am. Chem. Soc.* **2003**, *125*, 5610–5611.  
 (14) Kober, E. M.; Caspar, J. V.; Sullivan, B. P.; Meyer, T. J. *Inorg. Chem.* **1988**, *27*, 4587–4598.  
 (15) Williams, J. L. R.; Adel, R. E.; Carlson, J. M.; Reynolds, G. A.; Borden, D. G.; Ford, J. A., Jr. *J. Org. Chem.* **1963**, *28*, 387–390.

(16) Kim, D.; Shin, E. J. *Bull. Korean Chem. Soc.* **2003**, *24*, 1490–1494.  
 (17) van der Boom, M. E.; Richter, A. G.; Malinsky, J. E.; Lee, P. A.; Armstrong, N. R.; Dutta, P.; Marks, T. J. *Chem. Mater.* **2001**, *13*, 15–17.  
 (18) (a) Armelao, L.; Bertoncello, R.; Gross, S.; Badocco, D.; Pastore, P. *Electroanalysis* **2003**, *15*, 803–811. (b) Kim, Y.; Lee, H.; Dutta, P. K.; Das, A. *Inorg. Chem.* **2003**, *42*, 4215–4222.

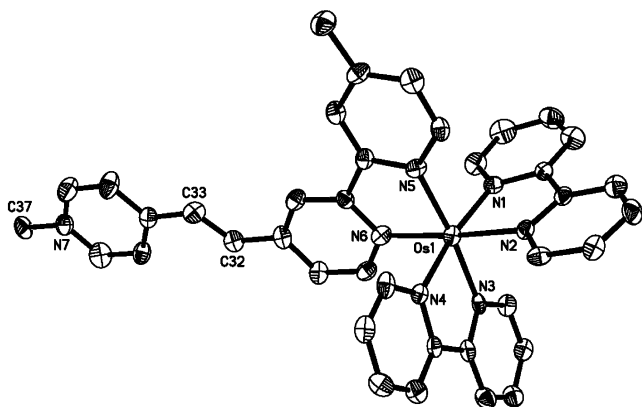


**Figure 1.** ORTEP diagram of complex **3**. (thermal ellipsoids set at 50% probability; counterions are omitted for clarity). Selected bond lengths [Å] and angles [deg]: Os(1)–N(1), 2.063(6); Os(1)–N(2), 2.061(6); Os(1)–N(3), 2.048(6); Os(1)–N(4), 2.052(6); Os(1)–N(5), 2.052(6); Os(1)–N(6), 2.047(6); C(37)–N(7), 1.484(9); C(32)–C(33), 1.328(11); N(6)–Os(1)–N(3), 96.3(2); N(6)–Os(1)–N(4), 86.5(2); N(3)–Os(1)–N(4), 78.2(2); N(6)–Os(1)–N(5), 78.1(2); N(3)–Os(1)–N(5), 173.9(2); N(4)–Os(1)–N(5), 98.8(2); N(6)–Os(1)–N(2), 174.7(2); N(3)–Os(1)–N(2), 89.0(2); N(4)–Os(1)–N(2), 94.2(2); N(5)–Os(1)–N(2), 96.6(2); N(6)–Os(1)–N(1), 101.2(2); N(3)–Os(1)–N(1), 97.7(2); N(4)–Os(1)–N(1), 171.6(2); N(5)–Os(1)–N(1), 86.0(2); N(2)–Os(1)–N(1), 78.4(2).

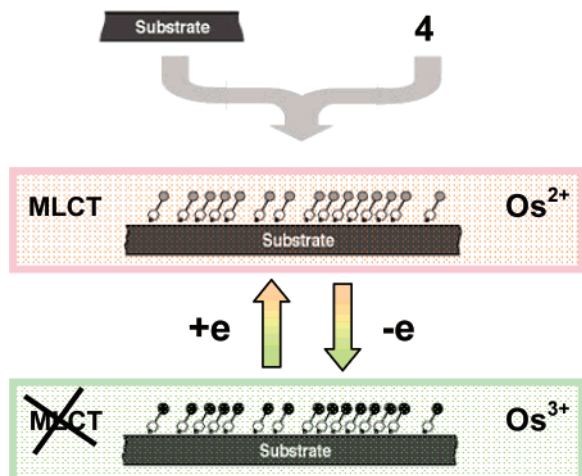


**Figure 2.** One step “wet-chemical” assembly of thermally robust osmium-based monolayers on glass and silicon substrate surfaces. Chemical redox ( $\text{Os}^{2+}/\text{Os}^{3+}$ ) switching was performed on glass substrates in air using acetonitrile solutions of ammonium hexanitratocerate(IV) as oxidizing and bis(cyclopentadienyl)cobalt as reducing agents.

material. UV/vis measurements on the functionalized glass substrates show that the new monolayers strongly adhere to the substrate surface as they cannot be removed by either the “Scotch tape decohesion” test or by a stream of critical carbon dioxide (snow jet).<sup>19</sup> The robustness of the monolayers is also illustrated by the thermal stability. Heating the monolayers assembled on glass substrates at 200 °C for 50 h in air with the exclusion of light showed no significant effect on the optical absorbance of the system, indicating that the molecular integrity and monolayer function are maintained even at these very high temperatures.

The new monolayers were characterized by a combination of aqueous contact angle measurements, semicontact atomic force microscopy (AFM), optical transmission (UV/vis), and ellipsometry. Aqueous contact angle measurements reveal

that  $\theta_a$  changes from  $<20^\circ$  for the freshly cleaned silicon substrate to  $65 \pm 4^\circ$  for the monolayer surface. Semicontact AFM measurements on monolayers grown on Si(100) substrates show an essentially smooth film surface. The root-mean-square surface roughness,  $R_q$ , is  $\sim 0.12$  nm for  $500 \text{ nm} \times 500 \text{ nm}$  scan areas (see Figure S1 in Supporting Information). Horizontal polymerization was not observed.<sup>20</sup> The UV/vis optical absorbance measurements of the monolayer on glass show the characteristic <sup>1</sup>MLCT and the triplet state of the metal-to-ligand charge transfer (<sup>3</sup>MLCT) bands at  $\lambda_{\text{max}} = 516$  and 692 nm, respectively. These results are comparable to the solution UV/vis spectra of **4** with red shifts of  $\Delta\lambda = +11$  nm and +2 nm for the <sup>1</sup>MLCT and <sup>3</sup>MLCT bands, respectively. Increasing the reaction time from 52 to 96 h does not affect the intensity and peak position of the MLCT bands, indicating the formation of a fully formed monolayer. Shortening the monolayer deposition time to 40 h decreases the intensity of both the <sup>1</sup>MLCT and the <sup>3</sup>MLCT bands. The average chromophore footprint of the covalent assembled monolayer on glass has been roughly estimated by UV/vis measurements to be  $\sim 60\text{--}70 \text{ \AA}^2/\text{chromophore}$ ,<sup>21</sup> which is as expected for this kind of molecular building block.<sup>22</sup> The ellipsometry-derived monolayer thickness is  $\sim 1.7$  nm. The estimated molecular length of complex **4** is  $\sim 2.1$  nm, indicating an average molecular tilt angle of  $\sim 17^\circ$  with respect to the surface normal. The packing density of chromophore **4** on the surface,  $V = 1.0\text{--}1.2 \text{ nm}^3$ , is approximately the packing density of the model complex **3** in the unit cell of the crystal structure ( $V = 2.0 \text{ nm}^3$  with two chromophores in one unit cell, see Table S1 in Supporting Information for details).

The monolayer redox chemistry on functionalized glass substrates was addressed using acetonitrile solutions of  $(\text{NH}_4)_2[\text{Ce}(\text{NO}_3)_6]$  (0.1 mM) and  $\text{Co}(\text{C}_5\text{H}_5)_2$  (1.0 mM) as oxidizing and reducing agents, respectively (Figure 2). The glass substrates were fully immersed into the solutions for 5 min in air and thoroughly rinsed with acetonitrile. The subsequent fully reversible optical changes have been observed with a standard double beam UV/vis spectrophotometer in the transmission mode (Figure 3). The <sup>1</sup>MLCT and <sup>3</sup>MLCT bands are significantly reduced upon oxidation of the  $\text{Os}^{2+}$  system, whereas these bands are fully restored upon reduction of the surface bound  $\text{Os}^{3+}$  complexes. The monolayer has to uptake and release additional counterions from the oxidation and reduction solutions to balance the charge. However, no significant shifts are observable which might indicate variation in molecular orientation, intermolecular interactions, solvent inclusion, and anion uptake/release. It is known that halide exchange can result in changes in monolayer linear and nonlinear optical properties<sup>23</sup> and

(19) Chow, B. Y.; Mosley, D. W.; Jacobson, J. M. *Langmuir* **2005**, *21*, 4782–4785.

(20) (a) Evmenenko, G.; van der Boom, M. E.; Yu, C.-J.; Kmetko, J.; Dutta, P. *Polymer* **2002**, *44*, 1051–1056. (b) Fadeev, A. Y.; McCarthy, T. J. *Langmuir* **2000**, *16*, 7268–7274.

(21) Durfor, C. N.; Turner, D. C.; Georger, J. H.; Peek, B. M.; Stenger, D. A. *Langmuir* **1994**, *10*, 148–152.

(22) (a) Shukla, A. D.; Strawser, D.; Lucassen, A. C. B.; Freeman, D.; Cohen, H.; Jose, D. A.; Das, A.; Evmenenko, G.; Dutta, P.; van der Boom, M. E. *J. Phys. Chem. B* **2004**, *108*, 17505–17511. (b) van der Boom, M. E.; Evmenenko, G.; Yu, C.; Dutta, P.; Marks, T. J. *Langmuir* **2003**, *19*, 10531–10537.

(23) Roscoe, S. B.; Yitzchaik, S.; Kakkar, A. K.; Marks, T. J.; Lin, W.; Wong, G. K. *Langmuir* **1994**, *10*, 1337–1339.

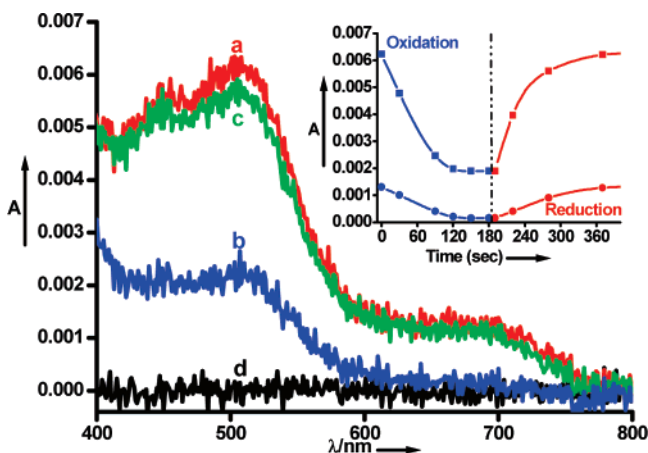


**Figure 3.** Representative absorption spectra for the redox-induced optical switching of the osmium-based monolayer on glass: (a)  $\text{Os}^{2+}$ , (b)  $\text{Os}^{3+}$ , (c)  $\text{Os}^{2+}$ , and (d) baseline. The inset shows follow-up measurements of the decrease (on oxidation with  $\text{Ce(IV)}$ ) and increase (on reduction with cobaltocene) of the absorbance vs time at  $\lambda(^{1}\text{MLCT}) = 516 \text{ nm}$  (■) and  $\lambda(^{3}\text{MLCT}) = 692 \text{ nm}$  (●).

surface wettability.<sup>24</sup> UV/vis follow-up measurements of the redox processes with time indicate that the metal centers are fully oxidized and reduced in  $\sim 3$  min under the above-mentioned reaction conditions (Figure 3, inset).

The simultaneous modulation of both  $^1\text{MLCT}$  ( $\sim 85\%$ ) and  $^3\text{MLCT}$  ( $\sim 98\%$ ) optical absorption bands with  $\lambda_{\text{max}} = 516$  and  $692 \text{ nm}$ , respectively, can be monitored by any given single wavelength in the  $400\text{--}750 \text{ nm}$  region. The optical modulation experiments can be conveniently interrupted at the  $\text{Os}^{2+}$  state and restarted without causing system instability. For example, cycling was stopped for 6 h after 5 cycles and for 24 h after 13 cycles as shown in Figure 4. Even after 25 redox cycles, no decay in the optical properties of the monolayer was observed.

The present study illustrates the straightforward chemical modulation of the optical absorbance of a thermally robust monolayer in air in the entire visible region by exploitation of the redox properties of a metal complex using common oxidizing and reducing agents. The monolayers are thermally robust, and 25  $\text{Os}^{2+}/\text{Os}^{3+}$  redox cycles have been demonstrated. The solution-surface electron transfer process induced

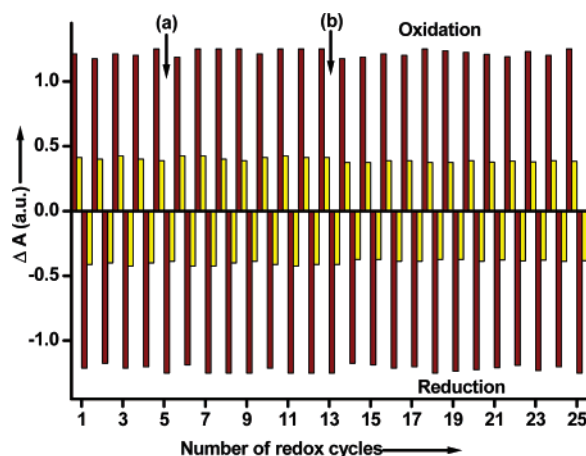


**Figure 4.** Representative chemical on/off switching of the  $^1\text{MLCT}$  and  $^3\text{MLCT}$  bands at  $\lambda = 516 \text{ nm}$  (brown) and  $692 \text{ nm}$  (yellow), respectively.  $\Delta A$  (in arbitrary units) vs the number of  $\text{Os}^{2+}/\text{Os}^{3+}$  redox cycles. Oxidation was carried out in an acetonitrile solution of ammonium hexanitratocerate(IV) (0.1 mM) while reduction was carried out in an acetonitrile solution of bis(cyclopentadienyl)cobalt (1.0 mM) (5 min each). Arrows indicate a break of 6 h after cycle 5 (a) and 24 h after cycle 13 (b).

changes in the molecular properties of the monolayer have been monitored by UV/vis transmission spectroscopy with a conventional spectrophotometer. The here-presented siloxane-based monolayers and surface chemistry may open new opportunities in interfacial engineering and the formation of monolayer-based memory devices and nonlinear/electro-optical switches. Addressing the metal oxidation state of ruthenium and iron complexes and the MLCT bands in solution is known to result in switching of the molecular second-order polarizability and fluorescence properties.<sup>11,25</sup> Future monolayer studies will involve modulation of these functions.

**Acknowledgment.** This research was supported by the Helen and Martin Kimmel Center for Molecular Design, MINERVA, BMBF, BIKURA, and the MJRG for Molecular Materials and Interface Design. M.E.v.d.B is the incumbent of the Dewey David Stone and Harry Levine career development chair.

**Supporting Information Available:** Formation and characterization data of compounds **2–4**, X-ray analysis procedure and data for complex **3** (Table S1), and monolayer formation and characterization with complex **4** (Figure S1; PDF). This material is available free of charge via the Internet at <http://pubs.acs.org>.

(24) Lee, B. S.; Chi, Y. S.; Lee, J. K.; Choi, I. S.; Song, C. E.; Namgoong, S. K.; Lee, S.-G. *J. Am. Chem. Soc.* **2004**, *126*, 480–481.

(25) (a) Hatzidimitriou, A.; Gourdon, A.; Devillers, J.; Launay, J.-P.; Mena, E.; Amouyal, E. *Inorg. Chem.* **1996**, *35*, 2212–2219. (b) Kober, E. M.; Sullivan, B. P.; Dressick, W. J.; Caspar, J. V.; Meyer, T. J. *J. Am. Chem. Soc.* **1980**, *102*, 7383–7385.